

The Irradiation Origin of Beryllium Radioisotopes and Other Short-lived Radionuclides

Matthieu Gounelle^{1,2,3}, Frank H. Shu⁴, Hsien Shang⁵, A. E. Glassgold⁶, K. E. Rehm⁷, Typhoon Lee⁸

ABSTRACT

Two explanations exist for the short-lived radionuclides ($T_{1/2} \leq 5$ Ma) present in the solar system when the calcium-aluminum-rich inclusions (CAIs) first formed. They originated either from the ejecta of a supernova or by the *in situ* irradiation of nebular dust by energetic particles. With a half-life of only 53 days, Beryllium-7 is then the key discriminant, since it can be made only by irradiation. Using the same irradiation model developed earlier by our group, we calculate the yield of ${}^7\text{Be}$. Within model uncertainties associated mainly with nuclear cross sections, we obtain agreement with the experimental value. Moreover, if ${}^7\text{Be}$ and ${}^{10}\text{Be}$ have the same origin, the irradiation time must be short (a few to tens of years), and the proton flux must be of order $F \sim 2 \times 10^{10} \text{ cm}^{-2} \text{ s}^{-1}$. The x-wind model provides a natural astrophysical setting that gives the requisite conditions. In the same irradiation environment, ${}^{26}\text{Al}$, ${}^{36}\text{Cl}$ and ${}^{53}\text{Mn}$ are also generated at the measured levels within model uncertainties, provided that irradiation occurs under conditions reminiscent of solar impulsive events (steep energy spectra and high ${}^3\text{He}$ abundance). The decoupling of the ${}^{26}\text{Al}$ and ${}^{10}\text{Be}$ observed in some rare CAIs receives a quantitative explanation when rare

¹Université Paris XI-Centre de Spectrométrie Nucléaire et de Spectrométrie de Masse (CSNSM), Bâtiment 104, 91 405 Orsay Campus, France

²Also at Impact & Astromaterials Research Center (IARC), Department of Mineralogy, Natural History Museum, London, UK

³Present address: Laboratoire d'Étude la Matière Extraterrestre, Muséum National d'Histoire Naturelle, 57 rue Cuvier, 75 005 Paris

⁴National Tsing Hua University, Hsinchu, Taiwan

⁵Institute of Astronomy and Astrophysics, Academia Sinica, Taipei, Taiwan

⁶Department of Astronomy, University of California, Berkeley, Berkeley, CA 94720-3411, USA

⁷Physics Division, Argonne National Laboratory Argonne, IL 60439, USA

⁸Institute of Earth Science, Academia Sinica, Taipei 115, Taiwan

gradual events (shallow energy spectra and low ^3He abundance) are considered. The yields of ^{41}Ca are compatible with an initial solar system value inferred from the measured initial $^{41}\text{Ca}/^{40}\text{Ca}$ ratio and an estimate of the thermal metamorphism time (Young et al. 2005), alleviating the need for two-layer protoCAIs. Finally, we show that the presence of supernova-produced ^{60}Fe in the solar accretion disk does not necessarily mean that other short-lived radionuclides have a stellar origin.

Subject headings: ^7Be , irradiation, early solar system, cosmic rays, x-wind, short-lived radionuclides, meteorites

1. Introduction

An important result concerning the formation of the solar system is the discovery that radionuclides with half-lives of the order of a million years (Ma) and less were alive when Calcium-Aluminum-rich Inclusions (CAIs) and chondrules, the igneous components of chondrites, were formed (see Russell, Gounelle & Hutchinson 2001 and McKeegan & Davis 2003 for recent reviews). Furthermore, some short-lived radioactivities, ^{10}Be ($T_{1/2} = 1.5$ Ma), ^{26}Al (0.74 Ma), ^{36}Cl (0.3 Ma), ^{41}Ca (0.1 Ma), ^{60}Fe (1.5 Ma) and possibly ^{53}Mn (3.7 Ma), existed at levels (see Table 1) well above the expectations of models of continuous galactic nucleosynthesis (e.g. Meyer & Clayton 2000). These findings have motivated two different kinds of explanations. The *external* model stipulates that the radionuclides were made in a supernova or in an asymptotic giant branch (AGB) star (e.g., Busso, Gallino & Wasserburg 2003). In the case of a supernova, it has been proposed that the expelled material triggered the collapse of a nearby molecular cloud core, which led to the formation of the solar system (Cameron & Truran 1977). More recently, an Orion-like environment has been suggested for the birth of the solar system (Hester et al. 2004). The *internal* irradiation model conjectures that the radionuclides were created by the irradiation of the solar environment by energetic protons, ^4He and ^3He nuclei, accelerated by gradual or impulsive events near an active young Sun (Lee et al. 1998; Goswami et al. 2001; Gounelle et al. 2001; Marhas et al. 2002; Leya et al. 2003). Thus, establishing the origin of the short-lived radionuclides can provide important constraints on the astrophysical setting of the Sun’s birth, stellar nucleosynthesis models, irradiation processes around young stellar objects, and early solar system chronology (Gounelle et al. 2005a,b; Kita et al. 2005).

Beryllium-7 decays to ^7Li with a half-life of 53 days. Because of this very short half-life, it must have an internal irradiation origin, since any ^7Be produced outside the nascent solar system would have decayed long before being incorporated into the first condensing

solids. While the mere discovery of ${}^7\text{Be}$ would be definite proof for *in-situ* irradiation, measurement of its abundance, together with that of other irradiation products such as ${}^{10}\text{Be}$ (McKeegan Chaussidon and Robert 2000), would provide important information concerning the irradiation conditions (duration as well as flux, energy spectra and isotopic composition of the accelerated particles).

The experimental detection of ${}^7\text{Be}$ has proven to be a long and difficult quest, largely because of the high mobility of its daughter element, Li. A hint of the presence of ${}^7\text{Be}$ was first seen in an Allende CAI (USNM 3515) at a high relative abundance, ${}^7\text{Be}/{}^9\text{Be} \sim 0.1$ (Chaussidon, Robert, & McKeegan 2002). However, a definitive isochron could not be established for this CAI, which has been highly disturbed by secondary events. Recently, Chaussidon, Robert & McKeegan (2004, 2005) identified 37 spots within Allende CAI 3529-41 for which the Li isotopic record has been undisturbed since crystallization. They determined a well-defined isochron for these 37 points and established that ${}^7\text{Be}$ was alive in the early solar system at a level ${}^7\text{Be}/{}^9\text{Be} = (6.1 \pm 1.3) \times 10^{-3}$ (2σ error).

The goal of this paper is to examine the yields of ${}^7\text{Be}$ in the context of the irradiation model we have developed over the past several years (Shu et al. 1996; Shu et al. 1997; Lee et al. 1998; Gounelle et al. 2001). We will establish additional constraints on irradiation models imposed by the presence of ${}^7\text{Be}$ and ${}^{10}\text{Be}$ in the early solar system. Calculations for the production of ${}^{36}\text{Cl}$, a newly discovered radionuclide (Lin et al. 2005) with a half-life of 0.3 Ma, are also presented, as well as new data and updated computations for ${}^{26}\text{Al}$, ${}^{41}\text{Ca}$ and ${}^{53}\text{Mn}$. We also discuss the implications of the high abundance of ${}^{60}\text{Fe}$ in the early solar system.

2. The Irradiation Model

2.1. Outline of the Model

We use the irradiation model in the form developed by Gounelle et al. (2001) to calculate the yield of ${}^7\text{Be}$. Their preferred case (c.f. Figure 2d of that paper) is adopted, and the parameters are kept the same except for the spectral index p and the ${}^3\text{He}/{}^1\text{H}$ ratio, which are varied within reasonable ranges. Case 2d refers to the geometry of the assumed core-mantle structure of protoCAIs: the minimum and maximum core sizes vary between 0.0050 and 2.5 cm, as natural CAIs do, and the mantle thickness is fixed at 0.28 cm (Shu et al. 2001). Here we provide the main characteristics of our model and discuss how it is implemented for the new calculations of ${}^7\text{Be}$ and ${}^{36}\text{Cl}$. The very short half-life of ${}^7\text{Be}$ (53 d vs \sim Ma for other radionuclides) calls for a special treatment. Additional details on the irradiation model may

be found in Gounelle et al. (2001).

Of basic importance in irradiation models are the *absolute* yields of the short-lived radionuclides. By absolute yield we mean the abundance of a radionuclide calculated relative to a fixed, stable-isotope reference (e.g. $^{26}\text{Al}/^{27}\text{Al}$), *not* abundances of radionuclides relative to one another. The absolute yields depend linearly on the product of the number flux of cosmic rays, F_{CR} , and the irradiation time, Δt . These quantities can vary over many orders of magnitude, depending on the astrophysical environment, implying changes in the short-lived-radionuclide yields of many orders of magnitude. Other parameters, like the composite structure of the targets, the shielding, or the cosmic ray properties, induce variations in the yields of the short-lived radionuclides that are no larger than a few orders of magnitude (Lee et al. 1998; Goswami et al. 2001; Gounelle et al. 2001; Marhas et al. 2002; Leya et al. 2003).

In our model, the number flux of protons is scaled to X-ray observations of young stellar objects (Lee et al. 1998), with $F_p (E \geq 10 \text{ MeV}) \sim 1.9 \times 10^{10} \text{ cm}^2 \text{ s}^{-1}$. The irradiation of proto-CAIs occurs within the reconnection ring (Lee et al. 1998), and the effective number of proton passages in the reconnection ring is $\mathcal{M} = 1.6$. The irradiation time depends linearly on the size of the proto-CAIs. With a typical irradiation time of 20 yr for a 1 cm protoCAI, the irradiation time varies between a few years and a few tens of years, since protoCAIs vary between 0.2805 and 2.78 cm (Gounelle et al. 2001; Shu et al. 2001). Homogenization of the irradiation products is assumed to take place through frequent evaporation-condensation episodes that, in a steady-state picture, erase the calculated differences of the yields between small and large CAIs. The final yield of a short-lived radionuclide is obtained by integrating the irradiation products over the size distribution of the total population of CAIs, reflecting the continuous homogenization of irradiation products made possible by the high frequency of large flares compared to the irradiation duration (Grosso et al. 1998; Wolk et al. 2005).

The differential distribution of protons, $N(E)$, is assumed to be a power-law in energy. The spectral index p in $N(E) \propto E^{-p}$ has a range between 2.7 and 5. The number of ^4He nuclei relative to protons is fixed at 0.1, but the $^3\text{He}/^1\text{H}$ ratio varies between 0 and 1. Impulsive events are characterized by relatively steep proton spectra (higher p) and large abundances of ^3He , while gradual events have shallower proton spectra (lower p) and smaller abundances of ^3He (Reames 1995). We envision two different structures for proto-CAIs, a core-mantle configuration and a homogeneous chondritic composition (Gounelle et al. 2001).

For the production of ^{36}Cl , we consider proton, alpha and ^3He induced reactions on a diversity of targets such as Cl, S and K. The adopted average chondritic abundance of Cl is 704 ppm (Lodders 2003) while the adopted median CAI abundance is 390 ppm (Sylvester et al. 1993).

For the production of ${}^7\text{Be}$ (and ${}^{10}\text{Be}$) we consider proton, alpha and ${}^3\text{He}$ induced reactions on ${}^{16}\text{O}$. Because its mean-life τ (76 days) is short compared to typical irradiation times Δt , ranging from a few years to a few tens of years, ${}^7\text{Be}$ yields need to be calculated by balancing spontaneous decay against production by spallation reactions. Thus, for ${}^7\text{Be}$, and any short-lived radionuclide for which $\tau \ll \Delta t$, the yield is the production rate times τ rather than times Δt , which applies when $\tau \gg \Delta t$.

2.2. Updated Cross Sections

The main new input data are the production cross sections shown in Figure 1 and Figure 2. The ${}^7\text{Be}$ cross sections are based on numerical simulations using fragmentation and Hauser-Feshbach codes and on experimental data points (indicated by circles) from Landolt & Börnstein (1994). The ${}^{10}\text{Be}$ -production cross-sections have been updated since the work of Gounelle et al. (2001). The ${}^{16}\text{O}(\text{p},\text{x}){}^{10}\text{Be}$ cross section is from Sisterson et al. (1997); the ${}^{16}\text{O}({}^4\text{He},\text{x}){}^{10}\text{Be}$ cross section is from the experimental study of Lange et al. (1995) that had been previously overlooked; and the ${}^{16}\text{O}({}^3\text{He},\text{x}){}^{10}\text{Be}$ cross section is from a new simulation.

The ${}^{36}\text{Cl}$ -producing cross sections (Figure 2) are based on numerical simulations using fragmentation and Hauser-Feshbach codes. In the absence of experimental data, the input model parameters have been chosen so that the calculations reproduce data obtained for lower and higher masses (e.g. Al, Ca, Fe) where some data exist. Because of the dependence of the cross sections on the structure of the nuclei involved, it is difficult to give precise uncertainties for these cross sections. From comparisons with experimental data for other reactions, we estimate an uncertainty of 50% for the maximum of the cross section and a factor of 2 for cross sections that are changing significantly with energy.

Most of the ${}^3\text{He}$ cross-sections used by Lee et al. (1998) and by Gounelle et al. (2001) for the production of short-lived radionuclides came from theoretical nuclear physics codes and not from direct laboratory measurements. To help reduce the uncertainties based on this over-reliance on theory, Fitoussi et al. (2004) measured the cross section for the reaction ${}^{24}\text{Mg}({}^3\text{He},\text{p}){}^{26}\text{Al}$ that is the main source of ${}^{26}\text{Al}$. In addition to using this experimentally determined cross section, we also include proton and alpha reactions for the production of ${}^{26}\text{Al}$ and ${}^{41}\text{Ca}$ that were previously ignored (for impulsive events) on the basis that their contributions to the ${}^{26}\text{Al}$ and ${}^{41}\text{Ca}$ yields were small compared with ${}^3\text{He}$. These cross sections are: ${}^{26}\text{Mg}(\text{p},\text{n}){}^{26}\text{Al}$, ${}^{27}\text{Al}(\text{p},\text{pn}){}^{26}\text{Al}$, ${}^{28}\text{Si}(\text{p},2\text{pn}){}^{26}\text{Al}$, ${}^{24}\text{Mg}(\alpha,\text{pn}){}^{26}\text{Al}$, ${}^{42}\text{Ca}(\text{p},\text{pn}){}^{41}\text{Ca}$, ${}^{40}\text{Ca}(\alpha,{}^3\text{He}){}^{41}\text{Ca}$, ${}^{40}\text{Ca}(\alpha,{}^3\text{H}){}^{41}\text{Sc}$, and they can be found in Lee et al. (1998).

To summarize, we now use an improved and a more complete set of cross sections

compared to Gounelle et al. (2001). Most of the key cross sections for the production of ${}^7\text{Be}$, ${}^{10}\text{Be}$ and ${}^{26}\text{Al}$ are now experimentally constrained. Among the cross sections important for our calculations, only ${}^{16}\text{O}({}^3\text{He},x){}^{10}\text{Be}$, ${}^{40}\text{Ca}({}^3\text{He},pn){}^{41}\text{Ca}$ as well as the ${}^{36}\text{Cl}$ producing cross sections lack experimental data. The uncertainties in the cross sections in Figure 1 (where experimental points are labeled with filled circles) are a factor of the order of a few, and possibly much larger for cross sections without experimental measurements such as the ones presented in Figure 2.

2.3. Results of the Calculations

Table 2 gives the calculated *absolute* yields of ${}^7\text{Be}$ as a function of the spectral index p and the ${}^3\text{He}/{}^1\text{H}$ ratio for two different cases: a core-mantle and a homogeneous chondritic compositional structure. The yields have been normalized to the experimental value obtained by Chaussidon, Robert and McKeegan (2005). Figure 3 shows the (relative) ${}^{10}\text{Be}/{}^7\text{Be}$ ratio as a function of the ${}^3\text{He}/{}^1\text{H}$ ratio for a range of values of the spectral index p . Using the *absolute* ${}^7\text{Be}$ yields in Table 2, this is equivalent to giving the *absolute* yield of ${}^{10}\text{Be}$. The result obtained with the same parameters as Gounelle et al. (2001), corresponding to ${}^3\text{He}/{}^1\text{H} = 0.3$ and $p = 4$, is marked by a filled circle in Figure 3.

Figure 4 shows the irradiation yields for the short-lived radionuclides of primary interest, ${}^7\text{Be}$, ${}^{10}\text{Be}$, ${}^{26}\text{Al}$, ${}^{36}\text{Cl}$, ${}^{41}\text{Ca}$, ${}^{53}\text{Mn}$, for the preferred parameters, $p = 4$ and ${}^3\text{He}/{}^1\text{H} = 0.3$, and for the two different target compositions (core-mantle and chondritic). Figure 5 presents the results for a variety of spectral parameters. The case $p = 2.7$ and ${}^3\text{He}/{}^1\text{H} = 0$ represents typical gradual flares, while the case $p = 4$ and $p = 5$ with ${}^3\text{He}/{}^1\text{H} = 0.3$ represents impulsive flares. We now discuss the implications of these results.

3. Discussion

3.1. The Irradiation Origin of ${}^7\text{Be}$

The detection of ${}^7\text{Be}$, with a half-life of 53 d, in meteorites (Chaussidon, Robert and McKeegan 2005) provides definitive evidence for *in situ* irradiation of pre-meteoritic solids and for local irradiation models. In fact, an earlier theoretical calculation, using preliminary cross section data (Gounelle et al. 2003), *predicted* the experimental result (Chaussidon, Robert & McKeegan 2004) to within a factor of two. An explanation of ${}^7\text{Be}$ in terms of some other process (e.g., Cameron 2003) is possible only if CAIs themselves formed outside the solar system and were never subsequently re-heated to reset the beryllium-lithium clock.

In such a case, however, the entire dating of the solar system, based on the nearly identical radiochemical ages of all CAIs, would be called into question.

For reasonable cosmic ray parameters (p ranging between 2.7 and 5, and ${}^3\text{He}/{}^1\text{H}$ ranging from 0 to 1), the ${}^7\text{Be}$ yields in Table 2 vary between 0.12 and 5.6 times the experimental value. The preferred model of Gounelle et al. (2001), with $p = 4$ and ${}^3\text{He}/{}^1\text{H} = 0.3$, gives ${}^7\text{Be}/{}^9\text{Be} = 7.5 \times 10^{-3}$, which compares favorably with the measured value of ${}^7\text{Be}/{}^9\text{Be} = 6.1 \times 10^{-3}$. As can be seen in Table 2, the ${}^7\text{Be}$ yields do not depend very much on the chemical composition of the target (usually no more than a few per cent). This is because they depend on the O/Be ratio, and refractory Be undergoes minimal chemical fractionation. Although the agreement between the model and the experimental value is very good, uncertainties in the model, especially in the nuclear cross sections (see section 2), call for caution.

A possible source for variations in the yields of ${}^7\text{Be}$ are fluctuations of the energetic particle flux. Because the relevant timescale for ${}^7\text{Be}$ synthesis is tens of days, ${}^7\text{Be}$ is more likely to be sensitive to such fluctuations than, say, ${}^{10}\text{Be}$ with a half-life of 1.5Ma. Significant X-ray flares are observed for Sun-like young stellar objects with ages in the 1-2 Ma range on the order of several days (Wolk et al. 2005). Thus ${}^7\text{Be}$ synthesis in natural samples is likely to be more variable than other short-lived radionuclides.

A basic reason for the good agreement between the present model calculations and experiment is that the production of ${}^7\text{Be}$ requires a high accelerated particle flux. As pointed out in §2), the yield of ${}^7\text{Be}$ with its short half-life does not depend on the irradiation time Δt but on the mean life τ . It also depends only moderately on the cosmic-ray parameters, as can be seen in Table 2. Consistent with the results in Table 2, the only way to produce ${}^7\text{Be}$ at a significant level is to have a high flux of accelerated particles. The value adopted by Gounelle et al. (2001) and used here, $F_p(E \geq E_{10}) \sim 1.9 \times 10^{10} \text{ cm}^2 \text{ s}^{-1}$, is consistent with the measured X-ray properties of Sun-like stars (e.g., Wolk et al 2005). Our local irradiation scenario is also naturally conducive to high accelerated-particle fluxes because the particles are confined to as well as produced within the reconnection ring (the irradiation zone) by strong magnetic fields (see 3.5).

3.2. The Case of ${}^{10}\text{Be}$

Our results for ${}^{10}\text{Be}$ are shown in Figures 3, 4 and 5. The calculated ${}^{10}\text{Be}/{}^7\text{Be}$ ratio depends moderately strongly on the cosmic-ray parameters (index p and ${}^3\text{He}/{}^1\text{H}$), when ${}^3\text{He}/{}^1\text{H} > 0.01$, as shown in Figure 3. The preferred model of Gounelle et al. (2001) gives a satisfactory account of the experimental ratio: $({}^{10}\text{Be}/{}^7\text{Be})_{\text{model}} = 0.88$ vs. $({}^{10}\text{Be}/{}^7\text{Be})_{\text{exp}} =$

0.16. The over-production of ^{10}Be by a factor of ~ 5 is not that large, given the uncertainties in the cross sections. Moreover, it is reduced if we use a somewhat steeper spectral index, e.g., $p = 5$ as shown in Figure 5. Alternatively, the ^{10}Be yield would be lower if the irradiation time was lower. However, this modification would also decrease the yields of other short-lived radionuclides such as ^{26}Al .

The ratio $^{10}\text{Be}/^7\text{Be}$ does not depend at all on the number flux (see section §2.1) and very little on the target composition (see Table 2). It depends mostly on the irradiation time, which is estimated in our 2001 model to be a few years to a few tens of years. The irradiation time is essentially the residence time for proto-CAIs of a certain size in the reconnection ring before ejection to asteroidal distances by the fluctuating X-wind (Shu et al. 2001). Such time scales are also suggested by observations of the intervals between knot-forming episodes in the optical jets of young stellar objects (Reipurth and Bally 2001). We cannot emphasize too strongly that the resulting *mechanical* model (Shu et al. 2001) yields in order-of-magnitude exactly the irradiation time to reproduce the $^{10}\text{Be}/^7\text{Be}$ ratio.

Desch, Connolly and Srinivasan (2004) have challenged the idea that ^{10}Be was formed in the solar system by irradiation. They argue instead that most of the solar system ^{10}Be originated as ^{10}Be nuclei in galactic cosmic rays stopped in the progenitor molecular cloud core. This conclusion depends sensitively on a number of assumptions made in their calculations, e.g., in the variation of the mass-column density $\Sigma(\varpi, t)$ in a collapsing molecular-cloud core, taken from an earlier numerical study by Desch & Mouschovias (2001). Desch et al. (2004) regard Σ as being spatially uniform, whereas Desch & Mouschovias (2001) found Σ to decrease considerably with increasing distance ϖ from the center of the cloud core. The core has a mass ($45 M_{\odot}$), significantly in excess of what is expected for the formation of a solar-mass star. Furthermore, the time scale for core formation and ^{10}Be accumulation is ~ 10 Ma, an order of magnitude longer than allowed by the statistics of nearby molecular cloud cores with and without embedded stars (e.g., Lee & Myers 1999). Even so, Desch et al. (2004) still need to increase the galactic cosmic ray flux relevant to present values by an *ad hoc* factor of 2 to produce enough ^{10}Be . The long evolutionary time also leaves no room for the injection into the nascent protosolar cloud of other short-lived radionuclides like ^{26}Al , ^{41}Ca and ^{53}Mn from a stellar event. Because of its *ad hoc* nature, the proposal of Desch, Connolly and Srinivasan (2004) has few advantages over the more common view that ^{10}Be has an in-situ irradiation origin (e.g., McKeegan, Chaussidon & Robert 2000; Gounelle et al. 2001; Marhas et al. 2002; Huss 2004).

3.3. The Co-production of ^{26}Al , ^{36}Cl , ^{41}Ca and ^{53}Mn

Our preferred model (case 2d of Gounelle et al. 2001) with $p = 4$ and $^3\text{He}/^1\text{H} = 0.3$ can reproduce within a factor of a few the measured solar system abundance of ^7Be , ^{10}Be , ^{26}Al , ^{36}Cl , ^{41}Ca and ^{53}Mn (the thick solid curve in Figure 5). Chlorine-36 is slightly under produced relative to its experimental value but, given the uncertainties of the model, the agreement is satisfactory. The adoption of a new *experimental* cross section for the reaction $^{24}\text{Mg}(^3\text{He},p)^{26}\text{Al}$ does not modify the yield of ^{26}Al by more than a factor of 2, keeping the production of this radio-isotope in line with what had been calculated using *theoretical* cross sections. Taking into account the previously ignored proton and ^4He induced cross sections for impulsive flares does not change the yields by more than ten percent. However, the adoption of an experimental cross section for $^{16}\text{O}(^4\text{He},x)^{10}\text{Be}$ has slightly increased the ^{10}Be yield, degrading the quality of the fit with the experimental data. Adoption of a somewhat steeper spectral index ($p = 5$ instead of $p = 4$, all other parameters remaining the same) would put ^{10}Be and ^{36}Cl in line with the measured solar system value. This would not change much the yields of the other short-lived radionuclides (Figure 5), except for ^{41}Ca discussed below.

The yields of all of the main short-lived radionuclides (including the newly calculated chlorine-36) are independent of composition except for ^{41}Ca , as may be seen in Figure 4. The low ^{41}Ca measured value, $^{41}\text{Ca}/^{40}\text{Ca} = 1.5 \times 10^{-8}$ (Srinivasan et al. 1994), can be reproduced by our model only when a core-mantle chemistry is adopted (Shu et al. 1997; Gounelle et al. 2001). However, there are hints that the solar system initial $^{41}\text{Ca}/^{40}\text{Ca}$ may have been considerably higher (McKeegan et al. 2004) than the presently measured value.

Recent experimental findings suggest that the initial $^{26}\text{Al}/^{27}\text{Al}$ ratio of the solar system was higher than the measured "canonical" value 4.5×10^{-5} (MacPherson et al. 1995), with an initial $^{26}\text{Al}/^{27}\text{Al}$ of the order $\sim 7 \times 10^{-5}$ (Young et al. 2002; Galy et al. 2004; Young et al. 2004). Subsequent redistribution of Mg isotopes within the CAI would then lead to an apparent initial ratio of 4.5×10^{-5} , i.e., the canonical value. Given the uncertainties of our irradiation model, an increase of $\sim 20\%$ in the initial $^{26}\text{Al}/^{27}\text{Al}$ ratio would not change the overall level of agreement between the calculations and the measurements. However, it might partly solve the overproduction of ^{41}Ca observed when a pure chondritic composition is adopted (Figure 5).

Calcium-41 decays into ^{41}K (see Table 2). If the K isotopes had been subjected to the same isotopic resetting as the Mg isotopes, this would mean that the initial $^{41}\text{Ca}/^{40}\text{Ca}$ ratio might have been higher by a factor of $(^{26}\text{Al}_{\text{initial}}/^{26}\text{Al}_{\text{reset}}) \frac{\tau(^{26}\text{Al})}{\tau(^{41}\text{Ca})} = (7/4.5) \frac{\tau(^{26}\text{Al})}{\tau(^{41}\text{Ca})} = 26$, where we have simply applied exponential decay law to both ^{26}Al and ^{41}Ca . It is therefore

very likely that the initial $^{41}\text{Ca}/^{40}\text{Ca}$ ratio was closer to 3.9×10^{-7} than to 1.5×10^{-8} . Such an early solar-system value would be consistent, within errors, with our computed irradiation yield of ^{41}Ca without the ad hoc adoption of a core-mantle structure (see Figure 6). Isotopic redistribution would be less important for other short-lived radionuclides because they have longer half-lives than ^{26}Al . Chlorine-36 could also have been higher by a factor of ~ 3.8 because of this thermal metamorphism, slightly degrading the good fit of Figures 5 and 6. Chaussidon, Robert and McKeegan (2005) have observed such a post-magmatic redistribution for Li isotopes, but have been able to deconvolve its effect from the ^7Be decay.

3.4. Decoupling of ^{26}Al and ^{10}Be

Mahas, Goswami & Davis (2002) have detected the past presence of ^{10}Be in some rare refractory inclusions containing calcium aluminum oxides known as hibonites in which ^{26}Al and ^{41}Ca (Sahjpal et al. 1998) are conspicuously absent. They interpret this “decoupling” between ^{10}Be and ^{26}Al (and ^{41}Ca) as contradicting irradiation models that simultaneously produce ^{10}Be , ^{26}Al and ^{41}Ca .

Hibonites from CM2 chondrites, which show this decoupling between ^{10}Be and ^{26}Al , share with FUN inclusions the property of bearing large isotopic anomalies in neutron-rich isotopes. Such FUN inclusions also formed with little initial ^{26}Al , a fact accounted for by Lee et al. (1998) who suggested that FUN CAIs never experienced the impulsive-flare events that are rich in ^3He before being ejected by the X-wind. However, CAIs that never enter the reconnection ring can still be exposed to gradual-flare events that occur at larger distances. Such gradual events are capable of producing large amounts of ^{10}Be without co-producing ^{26}Al (or ^{41}Ca), according to the results shown in Figure 5. Thus, the occurrence of rare CAIs containing abundant ^{10}Be but little ^{26}Al or ^{41}Ca may have an explanation in exposure to gradual but not impulsive events. We note that the anomalies in stable isotopes are not produced by irradiation and are probably of nucleosynthetic origin (Fahey et al. 1987a).

The recent measurement of ^{10}Be initial value in the hibonite HAL makes our hypothesis amenable to confrontation with experimental data. Mahas and Goswami (2003) have measured $^{10}\text{Be}/^9\text{Be}$ of $(8.0 \pm 3.3) \times 10^{-4}$ in HAL. Using $^{26}\text{Al}/^{27}\text{Al} = (5.4 \pm 1.3) \times 10^{-8}$ (Fahey et al. 1987b), we get $\frac{^{10}\text{Be}}{^9\text{Be}}/\frac{^{26}\text{Al}}{^{27}\text{Al}} = (8.1 \pm 4) \times 10^3$ for HAL. For gradual flares ($p = 2.7$ and $^3\text{He}/^1\text{H} = 0$), we obtain $\frac{^{10}\text{Be}}{^9\text{Be}}/\frac{^{26}\text{Al}}{^{27}\text{Al}} = 4.7 \times 10^3$. The agreement within errors between the measured and the calculated ratio of ratios, $\frac{^{10}\text{Be}}{^9\text{Be}}/\frac{^{26}\text{Al}}{^{27}\text{Al}}$, indicates that our model can successfully account for the decoupling between ^{26}Al and ^{10}Be measured by Mahas, Goswami and Davis (2002). Our model predicts that the $^7\text{Be}/^{10}\text{Be}$ ratio should be lower than normal in hibonites and FUN inclusions. For the sake of simplicity in the actual calculations, we have

assumed the same scaling of particle fluxes from X-ray observations for both gradual and impulsive events, but they could well be different. In other words, one should not deduce from Figure 5 that the *absolute* ^{10}Be abundance is expected to be higher in gradual events compared to impulsive events, or that the $^{10}\text{Be}/^9\text{Be}$ should be higher in FUN inclusions than in normal inclusions.

3.5. The Astrophysical Environment

Irradiation in the reconnection ring produces the relatively high energetic particles fluxes that characterize our model. It is in this region that the magnetic fields generated by the young star and the accretion disk reconnect and accelerate protons and helium nuclei to energies of order of 10 MeV or more. The reconnection ring is confined by magnetic fields that prevent the ionized particles from escaping. The short irradiation times used in the model correspond to the residence times of proto-CAIs calculated for the reconnection ring (Shu et al. 2001), and are in harmony with the time scales observed for jets from active young stellar objects. The absolute proton flux is obtained from the observed X-ray luminosities of young stellar objects using a normalization based on measurements of X-rays and particle fluxes for the contemporary active Sun. The X-ray luminosity of active young stellar objects estimated by Lee et al. (1998), and used by Gounelle et al. (2001) as well as in this paper, is supported by recent measurements of the X-rays emitted by young stellar objects in the Orion Nebula Cluster (ONC) by the *Chandra* satellite (Feigelson, Garmire, & Pravdo 2002; Wolk et al. 2005). The proton flux used in our irradiation calculations for the reconnection ring (cited above as $F_p(E \geq 10\text{MeV}) \sim 1.9 \times 10^{10} \text{ cm}^2 \text{ s}^{-1}$), corresponds to an X-ray luminosity of $\sim 5 \times 10^{30} \text{ erg s}^{-1}$ (Lee et al. 1998; Gounelle et al. 2001). This is in line with the median value for flares observed by Wolk et al. (2005), $L_X \sim 10^{31} \text{ erg s}^{-1}$ in an unprecedented Ms exposure by *Chandra* of the ONC. These flares occur on an average repetition time of several days. Much more luminous flares are observed on longer time scales of the order of one year. Of course these observations of flares in the ONC refer mainly to T Tauri stars with ages $\sim 1 - 2 \text{ Ma}$, whereas much of the irradiation most likely occurs earlier during a much more active stage of accretion. Following the discussion of Lee et al (1998), the flares in that epoch were probably even more powerful.

The irradiation model developed by Goswami, Marhas and Sahjpal (1998), and extended by Marhas, Goswami and Davis (2002), does not feature a favorable environment for the high particle fluxes needed to explain the Be isotopes. These authors choose the asteroid belt, 2-3 AU distant from the young Sun, as the place to irradiate meteoritic precursors by protons and alpha particles. Because they consider the rare hibonites that contain

irradiation-produced ^{10}Be and no ^{26}Al to be the first solar system solids to form (Sahjipal and Goswami 1998), irradiation in their model takes place well before the accretion disk was dissipated. Because a 10 MeV proton is stopped when it has encountered 0.2 gr cm^{-2} of matter (Reedy 1990), the flux at asteroidal distances is expected to be well below the level needed to form ^7Be and other short-lived radionuclides, especially when the inverse-square dilution of the stellar energetic particles is taken into account. The irradiation model developed by Leya, Halliday and Wieler (2003) adopts the x-wind model as a general framework for irradiation close to the young Sun, followed by wind-borne delivery of the irradiated materials to the asteroid belt. However, Leya et al. (2003) do not adopt a high energy particle flux or an irradiation time from observations or first principles, but calculate yields *relative* to the $^{10}\text{Be}/^9\text{Be}$ ratio.

3.6. The Stellar Origin of ^{60}Fe

Neutron-rich ^{60}Fe is almost impossible to synthesize in the internal irradiation scenario because of the low abundance of appropriate (neutron-rich) projectiles and targets (Lee et al. 1998). However, it is well known that Type-II supernovae can produce large amounts of ^{60}Fe (Timmes et al. 1995; Rauscher et al. 2002). Using updated nuclear reaction yields and improved stellar physics, Rauscher et al (2002) estimate that Type-II supernovae can synthesize between 2.4×10^{-5} and $16 \times 10^{-5} M_{\odot}$ of ^{60}Fe , depending on the mass of the progenitor, somewhat higher than Timmes et al. (1995), $0.29\text{-}10.5 \times 10^{-5} M_{\odot}$.

The initial solar system value of $^{60}\text{Fe}/^{56}\text{Fe}$ is relatively well constrained since it has now been identified in the silicate portion of chondrules that were presumably formed early in the history of the solar system (Tachibana & Huss 2003). Tachibana et al. (2005) estimate that the initial $^{60}\text{Fe}/^{56}\text{Fe}$ was $5\text{-}10 \times 10^{-7}$. Smaller previous estimates were inferred by Shukolyukov & Lugmair (1996), $^{60}\text{Fe}/^{56}\text{Fe} = 6 \times 10^{-8}$, from ^{60}Fe identified in planetary differentiates that formed relatively late. The Tachibana et al. (2005) value is compatible with the initial $^{60}\text{Fe}/^{56}\text{Fe} = 9.2 \times 10^{-6}$ estimated by Mostefaoui et al. (2005) from measurements in Semarkona troilite. Using a solar system abundance of ^{56}Fe , $^{56}\text{Fe}/^1\text{H} = 3.16 \times 10^{-5}$ (Lodders 2003), the initial ^{60}Fe content of the solar system lies between $0.95 \times 10^{-9} M_{\odot}$ and $1.9 \times 10^{-9} M_{\odot}$.

The updated ^{60}Fe yields for Type-II supernovae and the new initial ^{60}Fe content of the solar system have important implications for the origin of ^{60}Fe and other short-lived radionuclides. They indicate that a supernova can deliver enough ^{60}Fe to the solar system’s progenitor molecular cloud core to account for the measured value. Other short-lived radionuclides are not equally easily co-delivered at their initial abundances. The contribution

of a supernova, or any star, to the inventory of short-lived radionuclides in the early solar system can be characterized by a number of factors: the stellar yields, the mass fraction f of ejecta that is injected in the protosolar accretion disk, and the time interval Δ between nucleosynthesis and delivery. For example, consider the model SN25P of Rauscher et al. (2002) that produces $1.6 \times 10^{-4} M_{\odot}$ of ^{60}Fe by adopting an injection fraction $f = 1.4 \times 10^{-4}$ (2.8×10^{-4}) and a time interval $\Delta = 7$ Ma. By construction, such a supernova injects $0.95 \times 10^{-9} M_{\odot}$ ($1.9 \times 10^{-9} M_{\odot}$) of ^{60}Fe in the protosolar accretion disk, in line with the observed value. Such a supernova would also deliver ^{26}Al , ^{36}Cl and ^{41}Ca at levels well below the estimated abundances for the early solar system.

No stellar model yet published can inject into a model protosolar accretion disk the whole inventory of short-lived radionuclides (^{26}Al , ^{36}Cl , ^{41}Ca , ^{60}Fe). In his study of a specific $25 M_{\odot}$ supernova model that delivers ^{26}Al , ^{41}Ca and ^{60}Fe at the correct abundance, Meyer (2005) fails to deliver ^{36}Cl by two orders of magnitude. Moreover, even the highest-mass stars require at least two million years of normal stellar evolution before they supernova, and low-mass molecular cloud-cores that form sunlike stars in Orion-like environments (e.g., Hester et al. 2004) have disappeared before this time. Similarly, although specific nucleosynthetic models of AGB stars ($M = 1.5 M_{\odot}$ and $Z = Z_{\odot}/6$) have the potential to co-deliver ^{26}Al , ^{41}Ca and ^{60}Fe to the solar system, they fail to give ^{36}Cl by two orders of magnitude and do not produce any ^{53}Mn (Gallino et al. 2004). Moreover, the association of a molecular cloud core and an AGB star is an improbable astrophysical event (e.g., Kastner and Myers 1994). Contrary to what has been often argued (Zinner 2003; Hester et al. 2004), the presence of ^{60}Fe at a high level in the nascent solar system does not necessarily imply that ^{26}Al and other short-lived radionuclides also have a stellar origin. A wide range of supernovae, distant in space and time from the early solar system, can deliver high levels of ^{60}Fe without producing significant amounts of other short-lived radionuclides.

4. Conclusions

The discovery of ^7Be (half-life 53 days) has important implications for early solar-system processes. First it definitely establishes that irradiation took place at an early stage in its formation. Second, it requires high accelerated particle fluxes, F_p ($E \geq 10$ MeV) $\sim 2 \times 10^{10} \text{ cm}^2 \text{ s}^{-1}$. When the measurements of ^7Be are combined with those for ^{10}Be , short irradiation times of the order of a few years to a few tens of years are adduced. The model developed by Lee et al. (1998) and Gounelle et al. (2001) satisfy these demanding conditions for high accelerated particles fluxes and short irradiation times. Our irradiation model produces reasonable abundances for other short-lived radionuclides, such as ^{26}Al ,

^{36}Cl , ^{41}Ca and ^{53}Mn , as well as the Be isotopes. The overall scenario is also consistent with the evidence for energetic photo-irradiation of early solar system rocks from the mass-independent fractionation observed in stable sulfur and oxygen isotopes (Rai, Jackson, & Thiemens 2005).

The decoupling between ^{10}Be and ^{26}Al observed in a few rare CAIs can be accounted for by rare gradual events. For ^{41}Ca , a core-mantle chemistry is required if the initial value is as low as $^{41}\text{Ca}/^{40}\text{Ca} = 1.5 \times 10^{-8}$. If the initial abundance of ^{41}Ca were a factor of 25 higher, as suggested by McKeegan et al. (2004), its abundance could be accounted for, within the model uncertainties, by a homogeneous chondritic composition, rather than a core-mantle structure. As noted earlier by Lee et al. (1998), local irradiation models fail to produce ^{60}Fe at the measured early solar system level, $^{60}\text{Fe}/^{56}\text{Fe} = 5\text{-}10 \times 10^{-7}$ (Tachibana et al. 2005). A distant supernova is a likely origin for ^{60}Fe , as previously suggested by Lee et al. (1998). We note that recent updated models of supernova nucleosynthesis produce large amounts of ^{60}Fe relative to other short-lived radionuclides, implying that it is possible for supernovae to inject ^{60}Fe in the solar system without co-delivering other short-lived radionuclides.

The authors had illuminating discussions with K. D. McKeegan, M. Chaussidon, A. M. Davis, R. N. Clayton, E.D. Young and M.J. Pellin at the workshop *Meteorites and the Early Solar System* held at Taipei, Taiwan in December 2003. They would like to thank V. Tatischeff and J. Duprat for fruitful conversations, as well as an anonymous reviewer for comments that significantly improved the manuscript. This research has received support from the Programme National de Planétologie (M.G.), NASA Grant NAG5-12167 (A.G. and F.H.S.), the US Department of Energy, Office of Nuclear Physics, under Contract No. W-31-109-ENG-38 (KER), and by the Theoretical Institute for Advances Research in Astrophysics (TIARA) operated under Academia Sinica and the National Science Council Excellence Projects through grants number NSC 94-2752-M-007-001 and NSC 94-2112-M-007-051 (TL, FHS, and HS).

This is IARC publication number 2005-0831.

REFERENCES

- Birck, J.-L. & Allègre, C.-J. 1985, *Geophys. Res. Lett.*, 12, 745
- Busso, M., Gallino, R. & Wasserburg, G. J. 2003, *Publications of the Astronomical Society of Australia*, 20, 356
- Cameron, A. G. W. 2003, *ApJ*, 587, 327
- Cameron, A. G. W. & Truran, J. W. 1977, *Icarus*, 30, 447
- Chaussidon, M., Robert, F., McKeegan, K.D. 2002, *Lunar Planet. Sci. Conf.*, 33, 1563
- Chaussidon, M., Robert, F., McKeegan, K.D. 2004, *Lunar Planet. Sci. Conf.*, 35, 1568
- Chaussidon, M., Robert, F., McKeegan, K.D. 2005, *Geochim. Cosmochim. Acta*, In Press
- Desch, S.J., Mouschovias, T.C., 2001 *ApJ*, 550, 314
- Desch, S. J., Srinivasan, G. & Connolly Jr, H. C. 2004, *ApJ*, 602, 528
- Fahey, A. J., Goswami, J. N., McKeegan, K. D. & Zinner, E. K. 1987a, *Astrophysical Journal*, 323, L91
- Fahey, A. J., Goswami, J. N., McKeegan, K. D., & Zinner, E. 1987b, *Geochim. Cosmochim. Acta*, 51, 329
- Feigelson, E. D., Garmire, G. P. & Pravdo, S. H. 2002, *ApJ*, 584, 911
- Fitoussi, C., et al. 2004, *Lunar Planet. Sci. Conf.*, 35, 1586
- Gallino, R., Busso, M. & Wasserburg, G. J. 2004, *New Astronomy Reviews*, 48, 133
- Galy, A., Hutcheon, I. D. & Grossman, J. N. 2004, *Lunar Planet. Sci. Conf.*, 35, 1790
- Goswami, J. N. & Vanhala, H. A. T. 2000, in *Protostars and Planets IV*, ed V. Mannings, A. P. Boss & S. S. Russell (Tucson: University of Arizona Press), 963
- Goswami, J. N., Marhas, K. K. & Sahijpal, S. 2001, *ApJ*, 549, 1151
- Gounelle, M. & Russell, S. S. 2005a, *Geochim. Cosmochim. Acta*, 69, 3129
- Gounelle, M. & Russell, S. S. 2005b, in *Chondrites and the protoplanetary disk*, ed A. N. Krot, E. R. D. Scott & B. Reipurth (ASP Conference Series), 548

- Gounelle, M., Shang, H., Glassgold, A. E., Shu, F. H., Rehm, E. K. & Lee, T. 2003, *Lunar Planet. Sci. Conf.*, 34, 1833
- Gounelle, M., Shu, F. H., Shang, H., Glassgold, A. E., Rehm, E. K. & Lee, T. 2001, *ApJ*, 548, 1051
- Hester, J. J., Desch, S. J., Healy, K. R., and Leshin, L. A. 2004, *Science*, 304, 1116
- Huss, G. R. 2004, *Met. Planet. Sci.*, 39, 5087
- Huss, G. R. & Tachibana S. 2004, *Lunar Planet. Sci. Conf.*, 35, 1811
- Kita, N. T., Huss, G. R., Tachibana, S., Amelin, Y., Nyquist, L. E. & Hutcheon, I. D. 2005, in *Chondrites and the protoplanetary disk*, ed A. N. Krot, E. R. D. Scott & B. Reipurth 558
- Landolt-Börnstein 1994, (Berlin, Heidelberg, New York: Springer-Verlag), Vol. 13
- Lange, H.-J., et al. 1995, *App. Radiat. Isot.*, 46, 83
- Lee, C. W. & Myers, P. C. 1999, *ApJS*, 123, 233
- Lee, T. 1988, in *Meteorites and the Early Solar System*, ed J. F. Kerridge & M. S. Matthews (Tucson: Arizona University Press), 1063
- Lee, T., Papanastassiou, D. A. & Wasserburg, G. J. 1977, *ApJ*, 211, L107
- Lee, T., Shu, F. H., Shang, H., Glassgold, A. E. & Rehm, K. E. 1998, *ApJ*, 506, 898
- Leya, I., Halliday, A. N. & Wieler, R. 2003, *ApJ*, 594, 605
- Lin, Y., Guan, Y., Leshin, L. A., Ouyang, Z. & Wang, D. 2005, *PNAS*, 102, 1306
- Lodders, K. 2003, *ApJ*, 591, 1220
- MacPherson, G. J., Davis, A. M. & Zinner, E. K. 1995, *Meteoritics*, 30, 365
- Marhas, K. K. & Goswami, J. N. 2003, *Lunar Planet. Sci. Conf.*, 34, 1303
- Marhas, K. K., Goswami, J. N. & Davis, A. M. 2002, *Science*, 298, 2182
- McKeegan, K. D., Krot, A. N., Taylor, D. J., Sahijpal, S. & Ulyanov, A. A. 2004, *Met. Planet. Sci.*, 39, A66
- McKeegan, K. D. & Davis, A. M. 2003, in *Treatise on geochemistry*, ed H. Holland & K. Turekian (Oxford: Elsevier-Pergamon), 1, 431

- McKeegan, K. D., Chaussidon, M. & Robert, F. 2000, *Science*, 289, 1334
- Meyer, B. S. & Clayton, D. D. 2000, *Space Science Reviews*, 92, 133
- Meyer, B. S. 2005, in *Chondrites and the Protoplanetary Disk*, ed A. N. Krot, E. R. D. Scott & B. Reipurth (Proceedings of the Astronomical Society of the Pacific), 515
- Mostefaoui, S., Lugmair, G. W. & Hoppe, P. 2005, *ApJ*, 625, 271
- Rai, V. K., Jackson, T. L., & Thiemens, M. H. 2005, *Science*, 309, 1062
- Rauscher, T., Heger, A., Hoffman, R. D., & Woosley, S. E. 2002, *ApJ*, 576, 323
- Reames, D. V. 1995, *Rev. Geophys. Supp.*, 33, 585
- Reedy, R. C. 1990, *Lunar Planet. Sci. Conf.*, 21, 1001
- Reipurth, B. & Bally, J. 2001, *ARA&A*, 39, 403
- Russell, S. S., Gounelle, M. & Hutchison, R. 2001, *Phil. Trans. Royal Soc. A*, 359, 1991
- Sahijpal, S., Goswami, J. N., Davis, A. M., Grossman, L. & Lewis, R. S. 1998, *Nature*, 391, 559
- Shu, F. H., Shang, H., Glassgold, A. E. & Lee, T. 1997, *Science*, 277, 1475
- Shu, F. H., Shang, H. & Lee, T. 1996, *Science*, 271, 1545
- Shu, F. H., Shang, S., Gounelle, M., Glassgold, A. E. & Lee, T. 2001, *ApJ*, 548, 1029
- Shukolyukov, A. & Lugmair, G. W. 1996, *Meteoritics & Planetary Science*, 31 (Supp), A129
- Shukolyukov, A. & Lugmair, G. W. 1993, *Science*, 259, 1138
- Sisterson, J. M., Kim, M., Caffee, M. W. & Reedy, R. C. 1997, *Lunar Planet. Sci. Conf.*, 28, 1327
- Srinivasan, G. & Goswami, J. N. 1994, *Astrophysical Journal*, 431, L67
- Srinivasan, G., Sahijpal, S., Ulyanov, A. A. & Goswami, J. N. 1996, *Geochim. Cosmochim. Acta*, 60, 1823
- Sylvester, P. J., Simon, S. B. & Grossman, L. 1993, *Geochim. Cosmochim. Acta*, 57, 3763
- Tachibana, S. & Huss, G. R. 2003, *ApJ*, 588, L41

- Tachibana, S., Huss, G. R., Kita, N. T., Shimoda, H. & Morishita, Y. 2005, Lunar Planet. Sci. Conf., 36, 1529
- Timmes, F. X., Woosley, S. E., Hartmann, D. H., Hoffman, R. D., Weaver, T. A. & Matteucci, F. 1995, ApJ, 449, 204
- Young, E. D., Ash, R. D., Galy, A. & Belshaw, N. S. 2002, Geochim. Cosmochim. Acta, 66, 683
- Young, E. D., Simon, J. I., Galy, A., Russell, S. S., Tonui, E. & Lovera, O. 2005, Science, 308, 223
- Wolk, S. J., Hardnen, F. R., Flaccommio, E., Micela, G., Favata, F., Shang, H. & Feigelson, E. D. 2005, ApJ Supp, 160, 423
- Zinner, E. 2003, Science, 300, 265

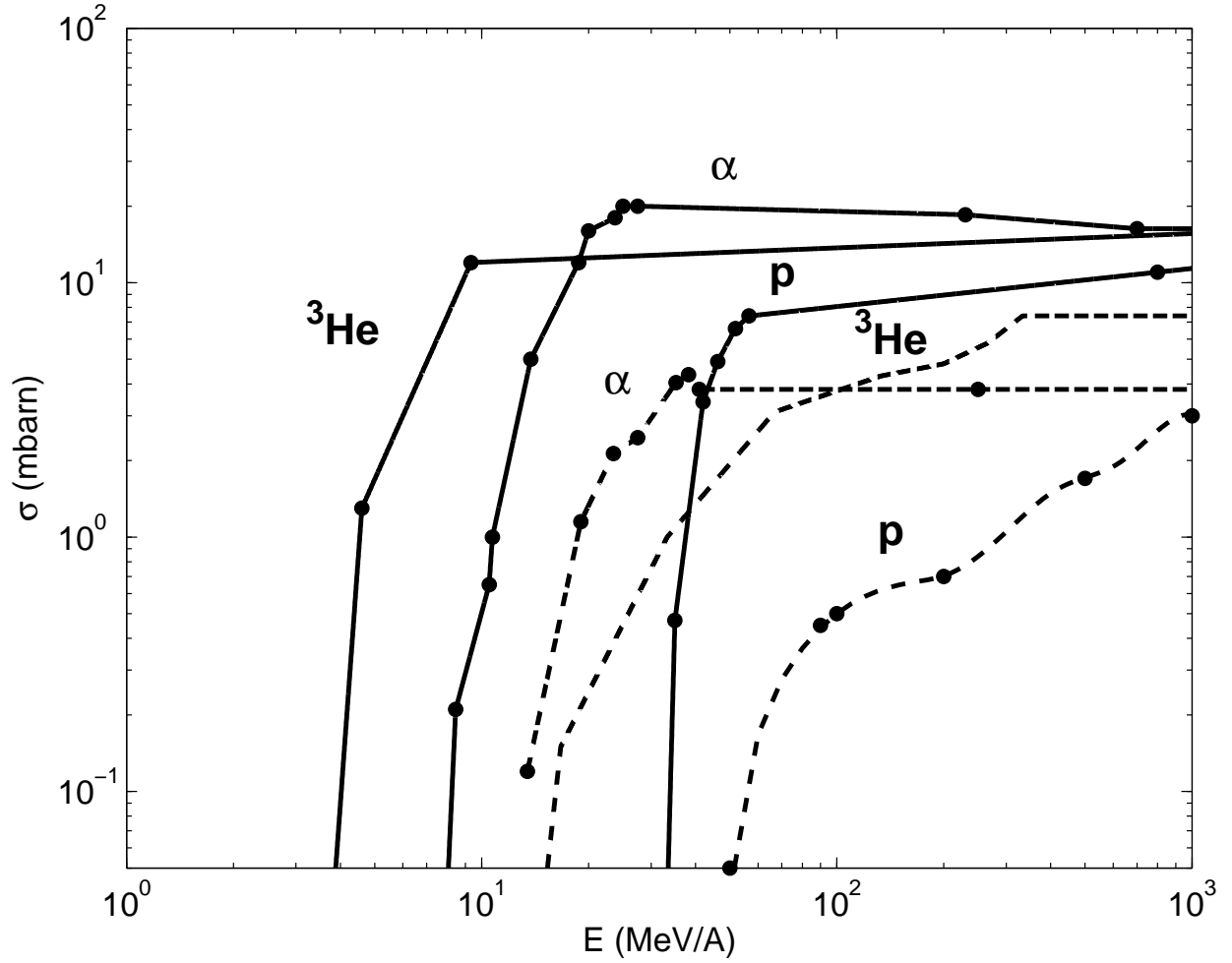


Fig. 1.— Adopted nuclear cross sections for the reactions ${}^{16}\text{O}(\text{CR},x){}^7\text{Be}$ and ${}^{16}\text{O}(\text{CR},x){}^{10}\text{Be}$. The solid curves are the ${}^7\text{Be}$ cross sections, and the dashed lines are the ${}^{10}\text{Be}$ cross sections. The incident projectiles, $\text{CR} = p, {}^3\text{He}$, and α are labelled on the graph. The nuclear cross sections are a combination of experimental data and Hauser-Feshbach fragmentation codes. Experimental data points are indicated by full black circles.

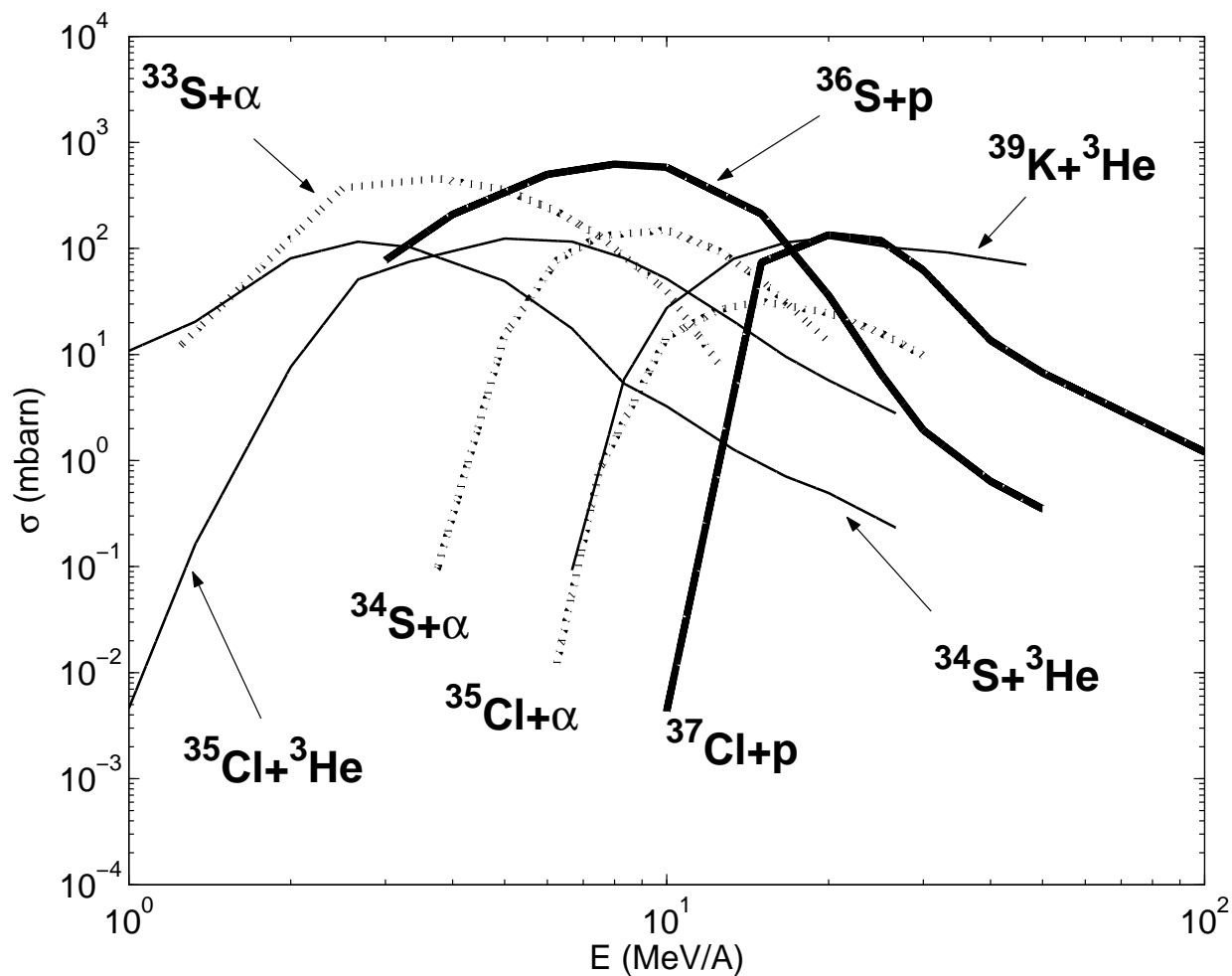


Fig. 2.— Adopted nuclear cross sections for the proton (thick line), α (dotted line) and ^3He (dashed line) induced reactions for the production of ^{36}Cl . The cross sections are based on numerical simulations using fragmentation and Hauser-Feshbach codes. In the absence of experimental data points, the input parameters have been chosen so that the calculations reproduce data obtained for lower and higher masses (e.g. Al, Ca, Fe) where some data exist.

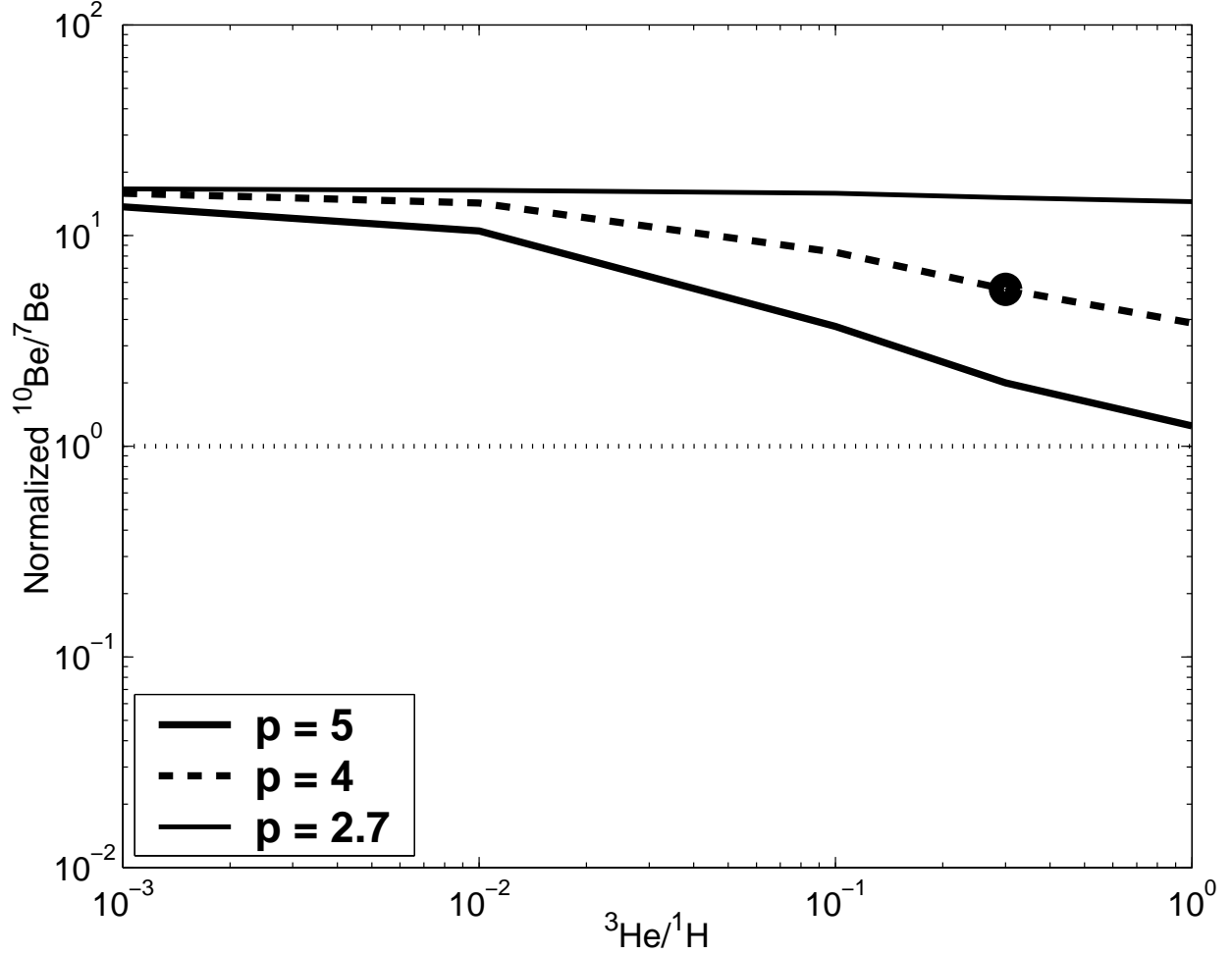


Fig. 3.— Plot of the $^{10}\text{Be}/^7\text{Be}$ ratio, normalized to the measured solar system value, as a function of the spectral parameter p and the $^3\text{He}/^1\text{H}$ abundance ratio. The horizontal dotted line denotes the experimental value calculated from Chaussidon, Robert and McKeegan (2005) and McKeegan, Chaussidon and Robert (2001). The filled circle corresponds to the preferred model of Gounelle et al. (2001), i.e with $p = 4$ and $^3\text{He}/^1\text{H} = 0.3$. As in the case of ^7Be (Table 2), the dependence on the target composition is weak and is not shown here.

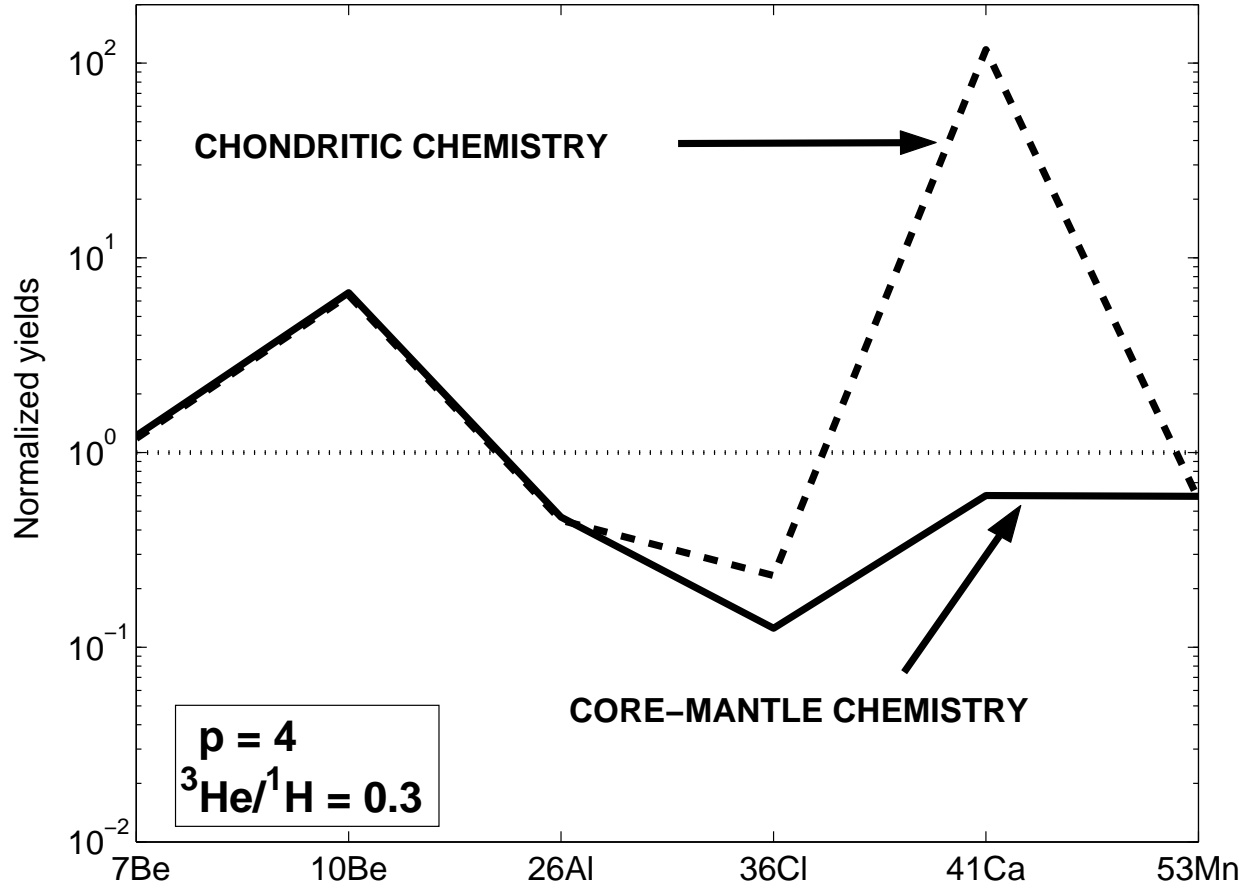


Fig. 4.— Yields of ${}^7\text{Be}$, ${}^{10}\text{Be}$, ${}^{26}\text{Al}$, ${}^{36}\text{Cl}$, ${}^{41}\text{Ca}$ and ${}^{53}\text{Mn}$ for fixed spectral parameters ($p = 4$, ${}^3\text{He}/{}^1\text{H} = 0.3$) and two different chemical compositions (core-mantle and chondritic). The yields are normalized to the experimental values (see Table 1), corresponding to the horizontal dotted line.

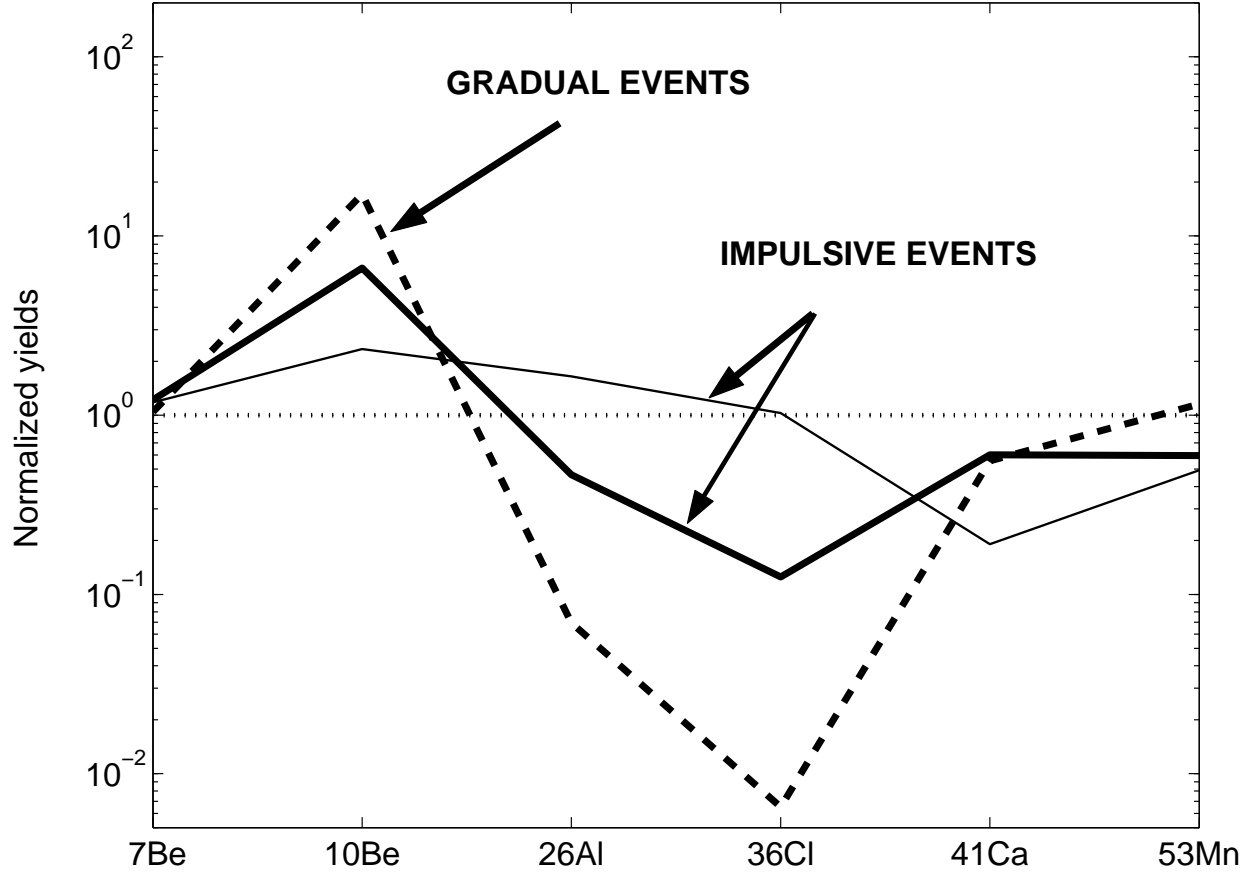


Fig. 5.— Yields of ${}^7\text{Be}$, ${}^{10}\text{Be}$, ${}^{26}\text{Al}$, ${}^{36}\text{Cl}$, ${}^{41}\text{Ca}$ and ${}^{53}\text{Mn}$ for fixed core-mantle structure (case 2d of Gounelle et al. (2001)) and a variety of spectral parameters. Impulsive flares have $p = 4$ (thick line) or $p = 5$ (thin line), and ${}^3\text{He}/{}^1\text{H} = 0.3$ while gradual flares have $p = 2.7$ and ${}^3\text{He}/{}^1\text{H} = 0$ (dashed line). The yields are normalized to the experimental values (see Table 1), corresponding to the horizontal dotted line.

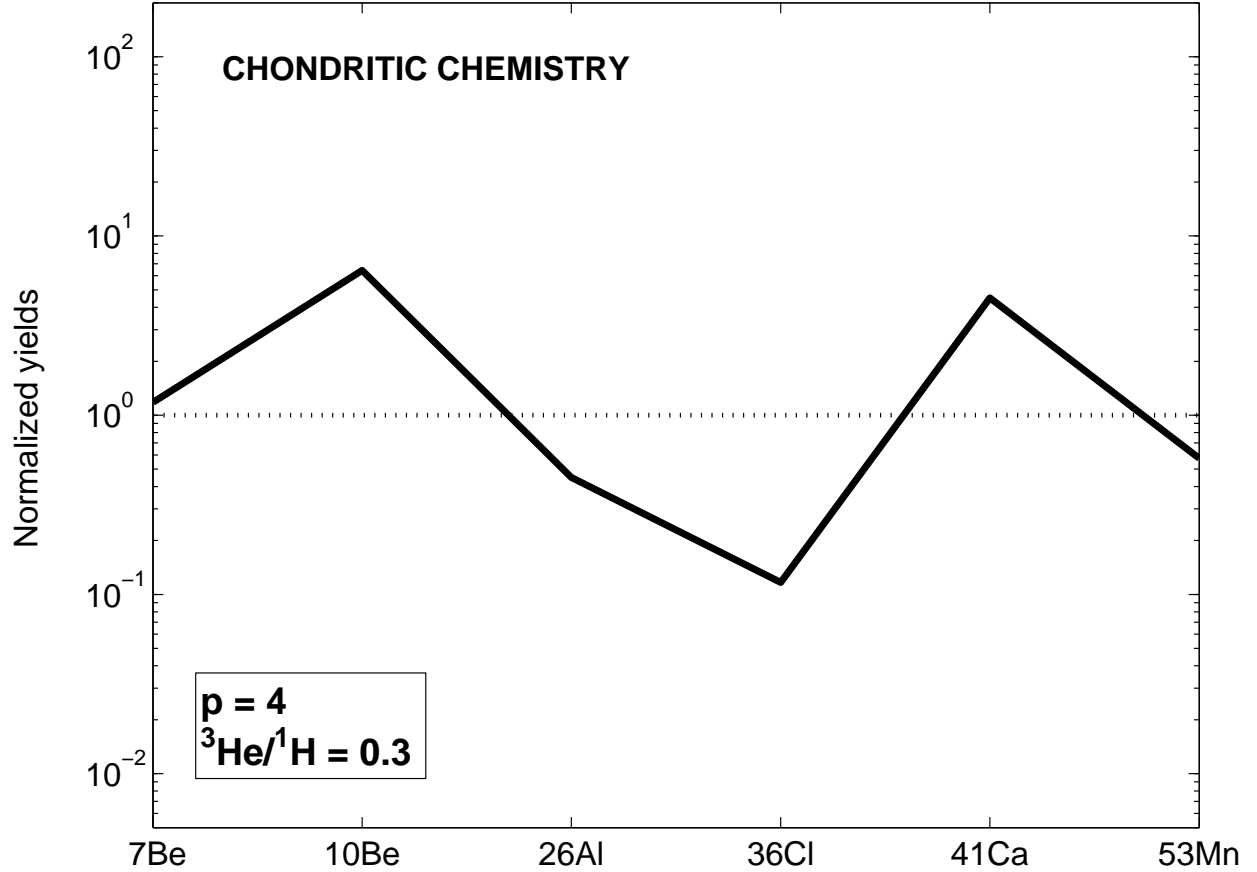


Fig. 6.— Yields of ${}^7\text{Be}$, ${}^{10}\text{Be}$, ${}^{26}\text{Al}$, ${}^{36}\text{Cl}$, ${}^{41}\text{Ca}$ and ${}^{53}\text{Mn}$ for a chondritic chemistry and the spectral parameters $p = 4$ and ${}^3\text{He}/{}^1\text{H} = 0.3$. The yields are normalized to the experimental values (see Table 1), corresponding to the horizontal dotted line. For ${}^{41}\text{Ca}$, we have adopted the initial value ${}^{41}\text{Ca}/{}^{40}\text{Ca} = 3.9 \times 10^{-7}$, more likely than the canonical ratio depicted in Table 1 (see text).

Table 1. Initial Values of Radionuclides Considered in the Present Paper.

R	$T_{\frac{1}{2}}$ (Ma)	D	S	R/S	ref
${}^7\text{Be}$	53 d	${}^7\text{Li}$	${}^9\text{Be}$	6.1×10^{-3}	a
${}^{41}\text{Ca}$	0.1	${}^{41}\text{K}$	${}^{40}\text{Ca}$	1.5×10^{-8}	b
${}^{36}\text{Cl}$	0.3	${}^{36}\text{S}$	${}^{35}\text{Cl}$	1.6×10^{-4}	c
${}^{26}\text{Al}$	0.74	${}^{26}\text{Mg}$	${}^{27}\text{Al}$	4.5×10^{-5}	d
${}^{10}\text{Be}$	1.5	${}^{10}\text{B}$	${}^9\text{Be}$	1×10^{-3}	e
${}^{60}\text{Fe}$	1.5	${}^{60}\text{Ni}$	${}^{56}\text{Fe}$	$5\text{-}10 \times 10^{-7}$	f
${}^{53}\text{Mn}$	3.7	${}^{53}\text{Cr}$	${}^{55}\text{Mn}$	4×10^{-5}	g

Note. — R, D and S stand respectively for the radionuclide of interest, its daughter and the stable reference isotope. The R/S values are observed or inferred in CAIs. The original solar system values may sometimes be higher (see text). (a) Chaussidon, Robert & McKeegan (2005). (b) Srinivasan et al. (1994). (c) Lin et al. (2005). (d) MacPherson, Zinner & Davis (1995). (e) McKeegan, Chaussidon & Robert (2000). (f) Tachibana et al. (2005); Mostefaoui, Lugmair & Hoppe (2005). (g) Birck & Allègre (1985).

Table 2. Variation of the Beryllium-7 Irradiation Yields with the Spectral Parameters.

	Core-mantle composition			Chondritic composition		
	p = 2.7	p = 4	p = 5	p = 2.7	p = 4	p = 5
${}^3\text{He}/{}^1\text{H} = 0$	1.0 (0)	2.3(-1)	9.6(-2)	9.9(-1)	2.2(-1)	9.3(-2)
${}^3\text{He}/{}^1\text{H} = 0.01$	1.1 (0)	2.6(-1)	1.3(-1)	1.0(0)	2.5(-1)	1.3(-1)
${}^3\text{He}/{}^1\text{H} = 0.1$	1.5(0)	5.6(-1)	4.5(-1)	1.4(0)	5.4(-1)	4.3(-1)
${}^3\text{He}/{}^1\text{H} = 0.3$	2.4(0)	1.2(0)	1.1(0)	2.3(0)	1.2(0)	1.1(0)
${}^3\text{He}/{}^1\text{H} = 1$	5.7(0)	3.5(0)	3.6(0)	5.5(0)	3.4(0)	3.5(0)

Note. — The ${}^7\text{Be}/{}^9\text{Be}$ ratio is normalized to its measured meteoritic value, ${}^7\text{Be}/{}^9\text{Be} = 6.1 \times 10^{-3}$. Except for the spectral parameters, all other parameters (irradiation time, cosmic-ray flux, etc.) are kept the same as in Gounelle et al. (2001) (see section 2.1). The bold type number corresponds to the preferred case of Gounelle et al. (2001) with $p = 4$ and ${}^3\text{He}/{}^1\text{H} = 0.3$.